

Gold nanoparticle based photometric determination of tobramycin by using new specific DNA aptamers

Xuyan Han, Yuhong Zhang, Jingjing Nie, Songyin Zhao, Yaping Tian, Nandi Zhou*

The Key Laboratory of Carbohydrate Chemistry and Biotechnology, Ministry of Education, School of Biotechnology, Jiangnan University, Wuxi 214122, China

*Corresponding author. Tel: +86-510-85197831; Fax: +86-510-85197831; E-mail:

zhounandi@jiangnan.edu.cn

Abstract

A magnetic bead-based SELEX was applied to identify 37 single-stranded DNA aptamers specific for tobramycin after ten rounds of selection. The aptamers were classified into nine families according to sequence analysis. Among them, several aptamers with typical sequences were selected and their dissociation constants (K_d s) were determined by a fluorescent method. An aptamer termed "Ap 32", with a K_d value of 56.88 ± 4.61 nM, possesses the highest affinity and satisfactory specificity. Theoretical modeling showed that nucleotides 14-18 and 26-29 play a most significant role in the interaction between aptamer and tobramycin. Subsequently, the sequence of Ap 32 was optimized through rationally designed truncation. The truncated aptamer Ap 32-2 consists of 34 nucleotides and has a K_d that is similar to the original one. It was chosen as the optimal aptamer for use in the assay and was immobilized on gold nanoparticle (AuNP). On addition of tobramycin, the color turns from red to purple. The findings were used to design a photometric assay (best performed at 520 nm) that has a linear response in the 100 nM to 1.4 μ M concentration range, with a 37.90 nM detection limit. The method was applied to the determination of tobramycin in (spiked) honey samples successfully.

Keyword: magnetic beads; single-stranded DNA aptamer; fluorescence; dissociation constant; SELEX; sequence truncation; detection.

Introduction

Tobramycin is an aminoglycoside antibiotic which acts effectively against a wide spectrum of gram-negative bacteria [1,2]. The mechanism of action stems from its ability to interfere with bacterial protein synthesis by irreversibly binding to a ribosome, and then cause damage to the cell membrane and cell death. Therefore, tobramycin has been widely used as a veterinary drug for therapeutic and prophylactic purposes [3,4]. However, if it is overcommitted, the remaining tobramycin may be transmitted to the environment and human body, which can cause a serious threat to human health [5]. Thus, the sensitive and accurate assay for tobramycin is very important in the field of clinical and environmental analysis, as well as food safety control. Similar with other antibiotics, the frequently used methods for detection of tobramycin residue in food products include microbiological assays [6], immunoassays [7], high-performance liquid chromatography (HPLC) [8] and capillary electrophoresis (CE) [9], *etc.* Generally, these methods are complicated, time-consuming and expensive, which cannot meet the requirements of fast, on-site detection.

Aptamers are mainly synthetic single-stranded DNA (ssDNA) or RNA, which can combine with a variety of targets including small organic molecules [10], peptides [11], proteins [12], ions [13], or even cells [14] and bacteria [15]. Folding into distinct three-dimensional shapes (G-quartet, hairpin, T-junction, *etc.*), aptamers can possess complementary conformation and therefore high specificity and affinity for their target molecules [16]. Aptamers take several distinguish priority over antibodies, such

as chemical stability, renewability, convenience in synthesis, and a wider spectrum of targets [17,18]. Since the establishment of systematic evolution of ligands by exponential enrichment (SELEX) strategy in 1990 by Ellington and Tuerk [19], a large number of aptamers for different targets have been reported. Several aptamers targeting antibiotics such as streptomycin [20], tetracycline [21], chloramphenicol [22], ofloxacin [23] have been screened. Then these aptamers have been further applied in the detection of antibiotics using different techniques, such as electrochemical [24, 25], colorimetric [26], fluorescent [27], chemiluminescent [28] and cantilever array [29] detection. Among those reported detections, gold nanoparticle (AuNP) attracted wide attention and was frequently used as the carrier of recognition elements or the probe to amplify the detection signal, due to its unique characteristics, including strong surface plasmon resonance absorption, high extinction coefficient, excellent electrical conductivity, huge specific surface area, and high biocompatibility [30]. Particularly, the aggregation and disaggregation, as well as the peroxidase-like activity of AuNP, which are accompanied by apparent color change, have been widely used in the configuration of sensors. The change of color offers such sensors visual and on-site analysis characteristics, which can achieve rapid detection without the use of complicated equipments.

An RNA aptamer for tobramycin was reported by Jiang *et al.* in 1998 [31]. However, its application in detection hasn't been explored much due to the poor stability and high-cost of RNA. The reported aptamer-based sensors so far are mainly concentrated on the usage of very few so-called "star aptamers", such as aptamers for

thrombin, ATP, cocaine, *etc.* To date, kanamycin-specific aptamer reported by Song *et al.* obtained the widest application among all the reported aptamers for antibiotics [32]. Generally, aptamers selected by SELEX have a typical length of 70-130 nucleotides [33], which are composed of fixed sequences at both ends and a random sequence in the center. Such aptamers usually contain unnecessary nucleotide fragments for their binding to targets, which may also introduce uncertainty in the formation of their 3-D structure and weaken its affinity for targets in different solution systems. Truncation of the aptamers can not only improve the binding between the targets and the aptamers, but also reduce cost in detection, and therefore is a critical post-SELEX process to obtain ideal and practicable aptamers.

Currently, three strategies have been applied to shorten the length of the aptamers. The first one is step-removing of the nucleotides from one end or both ends of the aptamers [34]. This strategy obtains the maximum possible candidates, however, leads to mass experiments at the mean time. Moreover, the optimal sequence cannot be deduced in case the binding sites of the aptamers towards the targets are not successive. The second strategy is a random truncation of the nucleotides following an empirical trial and error approach. For example, the flanked fixed sequences at both ends of the aptamers were sometimes removed directly and the remaining central random sequences were then used as the starting sequences for further optimization through step-truncation or point mutation [35]. This strategy is empirical and the results are difficult to be predicted. Nucleotides in fixed sequences can sometimes contribute to the binding between the aptamers and the targets. Thus the removing of

the fixed sequences completely changes the conformation of the aptamers. The third strategy is rationally designed truncation of the nucleotides [36]. Briefly, the truncation is based on homologous alignment, consensus secondary structure analysis, and 3-D molecular docking. Since the truncation of the sequences is accurately designed, this strategy can greatly reduce the workload during the optimization and efficiently deduce the ideal aptamers.

We reported the selection of ssDNA aptamers with high affinity and specificity for tobramycin from a randomized library by SELEX. During the post-SELEX truncation, a rationally designed strategy was used, and an optimal aptamer with the length of 34 nucleotides was finally screened. The practicability of the aptamer was verified by the application in an AuNP-based photometric assay of tobramycin. The method was further used to detect tobramycin in honey samples.

Experimental

Chemicals and materials

Tobramycin sulfate, gentamicin sulfate, neomycin sulfate, kanamycin sulfate, streptomycin sulfate, and tetracycline hydrochloride were purchased from Sangon Biotech Co. Ltd (Shanghai, China) (<http://www.sangon.com>). Streptavidin magnetic beads and epoxy magnetic beads were purchased from Tianjin Chemical Regent Company (Tianjin, China) (<http://www.qiuhuan.com>). All PCR reagents were procured from TaKaRa Bio Inc (Dalian, China) (<http://takara.company.lookchem.cn>). Honey was purchased from the local supermarket.

The initial ssDNA library and PCR primers were synthesized and HPLC purified by Sangon Biotech Co. Ltd. The random ssDNA library (5'-TAGGGAATTCGTCGACGGATCC-N35-CTGCAGGTCGACGCATGCGCCG-3') contains a central random sequence of 35 nucleotides (nt), flanked by two primer binding sequences [37]. A forward primer (5'-TAGGGAATTCGTCGACGGAT-3') and a biotinylated reverse primer (5'-biotin-CGGCGCATGCGTCGACCTG-3') were used for PCR amplification and ssDNA generation. All the DNA sequences were dissolved in water to the concentration of 100 μ M.

All other chemicals were of analytical grade. Ultrapure water (18.2 M Ω cm) was used to prepare all aqueous solutions throughout the experiments.

Apparatus

Bio-Rad T100 Thermal Cycler (Bio-Rad Co., U.S.A.) was used for PCR amplification. NanoDrop 2000 Spectrophotometer (Thermo Fisher Scientific, Co., U.S.A.) was used to determine the concentration of all oligonucleotides. Enspire 2300 (Perkin Elmer, U.S.A.) was used for fluorescence intensity measurement. UV-visible absorption spectra were recorded with a UH5300 spectrophotometer (Hitachi, Japan).

Modification of epoxy magnetic beads

Epoxy magnetic beads were used for covalent immobilization of tobramycin. Firstly, 200 μ L (1.0 mg) epoxy magnetic beads were washed five times with 100 mM phosphate buffered saline (PBS, pH 8.0), then added into 200 μ L of 10 mM

tobramycin solution. The mixture was incubated at 30 °C for 16 h with mild shaking. The tobramycin-coated beads were washed five times with PBS and the residual free epoxy groups on the surface of the beads were blocked by incubation with 0.5 M ethanolamine (pH 8.0) at 30 °C for 8 h with mild shaking. Finally, the tobramycin-coated beads were washed and resuspended in 200 µL PBS and stored at 4 °C prior to use.

To evaluate the specificity of the selected aptamers, other antibiotics including streptomycin, neomycin, kanamycin, gentamicin, and tetracycline were immobilized onto the surface of epoxy magnetic beads, respectively, by using the same method as the immobilization of tobramycin.

***In vitro* selection**

To screen tobramycin-specific aptamers, multiple rounds of *in vitro* selection were carried out. In the first round, the tobramycin-coated magnetic beads were washed for five times with binding buffer (20 mM Tris-HCl containing 100 mM NaCl, 1 mM CaCl₂, 2 mM MgCl₂, 5 mM KCl and 0.02% Tween-20, pH 7.6). The initial ssDNA library (300 pmol) was denatured in binding buffer at 90 °C for 10 min, then cooled on ice for 10 min, and stood at room temperature for 5 min. Then the ssDNA was incubated with the tobramycin-coated magnetic beads for 1 h with mild shaking at room temperature. During the incubation, ssDNA sequences with affinity for tobramycin combined with tobramycin immobilized on the magnetic beads, while other ssDNA sequences kept free in the solution. After that, the magnetic beads were

washed for five times with binding buffer to completely remove unbound oligonucleotides. In order to recover the adsorbed ssDNA from the magnetic beads, the beads were incubated in 150 μL elution buffer (40 mM Tris-HCl containing 3.5 M urea, 10 mM EDTA and 0.02% Tween-20, pH 8.0) at 80 $^{\circ}\text{C}$ for 20 min with mild shaking. This procedure was repeated three times to ensure that all adsorbed ssDNA sequences were eluted.

The ssDNA eluted in solution was extracted with equal volume of phenol/chloroform/isoamylol (25:24:1), precipitated by addition of 1/10 volume of sodium acetate and 2.5 volume of ethanol and keeping in freezer for 2 h at -20 $^{\circ}\text{C}$, and then centrifuged at 10,000 rpm for 15 min at 4 $^{\circ}\text{C}$. The precipitated ssDNA was washed with 75% ethanol and dissolved in 10 μL sterile water. The concentration of ssDNA was detected by NanoDrop 2000 spectrophotometer. And then the ssDNA selected was amplified by PCR. 25 μL PCR reaction mixture contained 2 μL dNTP (2.5 mM), 1 μL forward primer (10 μM), 1 μL biotinylated reverse primer (10 μM), 0.1 μL Taq DNA polymerase (2.5 $\text{U}\cdot\mu\text{L}^{-1}$), 1 μL template ssDNA, 2.5 μL 10 \times PCR buffer and 17.4 μL double distilled water. PCR was conducted by denaturation at 95 $^{\circ}\text{C}$ for 30 s, annealing at 55 $^{\circ}\text{C}$ for 1 min and elongation at 72 $^{\circ}\text{C}$ for 1 min. The first cycle had an extended denaturation at 95 $^{\circ}\text{C}$ for 5 min. The final elongation step was extended at 72 $^{\circ}\text{C}$ for 5 min. By this means, the complementary strands of ssDNA with a biotin labeling were produced. The PCR products were confirmed by gel electrophoresis by using 3% agarose.

With the purpose of obtaining ssDNA sequences for the next round of selection,

streptavidin-modified magnetic beads were used to remove biotinylated complementary strands from double-stranded DNA. 25 μ L streptavidin-modified magnetic beads were washed with binding and washing (B&W) buffer (10 mM Tris-HCl containing 2 M NaCl and 1 mM EDTA, pH 7.5) for three times and suspended in 80 μ L B&W buffer. After that, 20 μ L PCR products were added to the solution and incubated at room temperature for 2 h. Then the beads were washed with B&W buffer, followed by the elution of ssDNA for two times with 30 μ L of 0.1 M NaOH at 37 °C for 2 h. During the dehybridization of double-stranded DNA in NaOH, the biotinylated complementary strands kept binding to streptavidin-modified magnetic beads, while the non-biotinylated ssDNA sequences were eluted from the beads. The concentration of ssDNA obtained was detected by NanoDrop 2000 spectrophotometer. Then obtained ssDNA was used as a secondary ssDNA pool for the next round.

Cloning, sequencing and structural analysis

The recovered ssDNA from the last round of SELEX was amplified by PCR with non-biotinylated primers. Then the PCR product was cloned and sequenced. These sequences were analyzed using DNAMAN software. The secondary structures of the aptamers were predicted by using the Mfold software. Molecular docking was performed to predict the binding motif between the aptamer and tobramycin by using Autodock 4.0 software.

Evaluation of the aptamers

The dissociation constants of the sequenced aptamers were determined by fluorescence analysis [38]. Firstly, the tobramycin-coated magnetic beads were washed with binding buffer for five times. Then different concentrations of the FAM-labeled aptamers were added in 200 μ L binding buffer, followed by denaturing at 90 °C for 10 min, immediately cooling on ice for 15 min, and then incubated with the washed beads for 2 h with mild shaking at room temperature. The unbound ssDNA was removed through washing five times with binding buffer. ssDNA which bound to tobramycin-coated beads was eluted with 200 μ L elution buffer at 80°C for 20 min with mild shaking, then the fluorescence intensity was measured by fluorescence spectrophotometer at 515 nm (excitation wavelength 490 nm). Binding affinity is expressed by the ratio of the fluorescence intensity of the binding ssDNA and the initially added ssDNA. The affinity of the aptamers for tobramycin was estimated by dissociation constant (K_d), which was calculated by fitting the data points by using the non-linear regression analysis and GraphPad Prism 5.0 software: $y = B_{\max} \cdot [\text{free ssDNA}] / (K_d + [\text{free ssDNA}])$, where y represents degree of saturation, B_{\max} represents the maximum number of binding sites, and $[\text{free ssDNA}]$ is the concentration of the unbound ssDNA [39].

To evaluate the specificity of the selected aptamers, different antibiotics such as neomycin, streptomycin, kanamycin, gentamicin, and tetracycline were coupled with the epoxy magnetic beads. These antibiotics modified beads were washed with binding buffer for five times before use. 200 pmol aptamers were added in 200 μ L

binding buffer, and the mixtures were denatured at 90 °C for 10 min, immediately cooled on ice for 15 min, and then mixed with different antibiotics modified beads respectively for 2 h with mild shaking at room temperature. Free ssDNA was removed through washing five times with binding buffer. The bound aptamers were eluted with 200 µL elution buffer at 80 °C for 20 min with mild shaking. The process was repeated three times to elute all bound ssDNA, whose concentration was then determined by NanoDrop 2000 spectrophotometer.

Detection of tobramycin using aptamer and AuNP-based photometric assay

To demonstrate the potential use of the screened aptamer in tobramycin detection, the widely reported AuNP-based photometric assay was carried out. AuNP were prepared as described previously [40]. 50 µL AuNP (17.5 nM) was incubated with 100 µL of 150 nM aptamer for 1 h at room temperature. Then 50 µL of different concentrations of tobramycin ranging from 0 to 1400 nM was added to the above mixture, respectively, followed by additional 50 min incubation at room temperature. Finally, 50 µL of 120 mM NaCl was added, and the UV-visible spectra of the mixture were recorded. The absorbance at 520 nm was used to quantify the concentration of tobramycin.

To prove the practicability of the assay, artificially contaminated honey samples were prepared by spiking different concentration of standard tobramycin solution into tobramycin-free honey. These honey samples were diluted for ten times with binding buffer before detection. Then 50 µL diluted honey samples containing different

concentration of tobramycin were used for testing, and the AuNP-based photometric assay was carried out as described above.

Results and discussion

***In vitro* selection**

Magnetic bead-based SELEX was carried out to screen ssDNA aptamers specific to tobramycin from a 79-mer initial ssDNA library including 35 random nucleotides. During the selection, the recovery of ssDNA binding to tobramycin-coated magnetic beads, which reflects the efficiency of the enrichment of the affinity, was monitored in each round. The definition of recovery is the ratio of the bound ssDNA to the magnetic beads and ssDNA in the pool of each round. As shown in Fig. 1, the recovery of ssDNA continuously increases from the first round to the eighth round of selection. However, it no longer increases after eight rounds of selection, indicating the saturation of the enrichment of the tobramycin-specific aptamers. Finally, aptamers obtained after ten rounds of selection were amplified by PCR and then cloned and sequenced.

Insert Fig. 1

Characterization of the selected aptamers

After cloning and sequencing, a total of 37 positive clones were identified and sequenced (Sangon Biotech Co. Ltd., Shanghai, China). From sequence analysis, some conserved motifs including “TTG”, “TGG”, “GGT” and “GTT” frequently

appear in the variable regions of these aptamers. Based on their homology, these aptamers were classified into 9 different families, as shown in Table S1.

The secondary structures of the aptamers were predicted by using the Mfold software. Among the predicted results, aptamers encoded Ap 1, Ap 11, Ap 12 and Ap 32 have similarity in their secondary structures, as shown in Fig. 2. In the mimic diagrams, green regions represent the fixed sequences and the black regions represent random sequences. At least three stem-loop patterns can be identified in these secondary structures, which may be significant for their binding to tobramycin. And the fixed sequences at both ends of the aptamers are apparently involved in the formation of these secondary structure patterns.

Insert Fig. 2

The affinity of the aptamers for the targets is undoubtedly one of the most important parameters of the aptamers, which is usually expressed in dissociation constant (K_d). To evaluate the affinity of the selected aptamers, binding affinity assay was performed by the fluorescent method. By non-linear regression analysis, the K_d values of Ap 1, Ap 11, Ap 12 and Ap 32 were determined to be 146.20 ± 13.72 nM, 96.87 ± 16.00 nM, 113.50 ± 19.37 nM and 56.88 ± 4.61 nM, respectively. The non-linear regression curves of the aptamers are shown in Fig. S1A. The values of B_{max} , which is another parameter in non-linear regression, were also determined and listed in Table S2. Among the tested aptamers, Ap 32 shows the lowest K_d value, *i.e.* the highest affinity for tobramycin, and therefore was chosen for further characterization and optimization.

Then the specificity of Ap 32 was investigated through determination and comparing of its recovery from tobramycin, streptomycin, neomycin, kanamycin, gentamicin and tetracycline modified magnetic beads. The results are shown in Fig. S1B. 76.6% of Ap 32 binds to tobramycin modified beads and subsequently recovers during elution, while the recoveries of Ap 32 from other antibiotics modified beads are all below 10%. Therefore, Ap 32 has both high affinity and high specificity to tobramycin.

Structural analysis and truncation of the aptamer

Although the affinity and specificity of Ap 32 are basically satisfactory, the 79-mer length of the sequence limits its potential application to a certain extent. Truncation of the aptamer through removing the redundant sequence based on structural analysis and rational design can help us obtain the optimized aptamers. The molecular docking was performed to predict the binding motif between Ap 32 and tobramycin by using Autodock 4.0 software. The simulated modeling is shown in Fig. 3, which indicates that nucleotides 14-18 and 26-29 in Ap 32 serve as recognition sites for tobramycin.

Insert Fig. 3

Based on the predicted secondary structure and the binding sites of the simulated modeling, two truncated aptamers Ap 32-1 and Ap 32-2, with the length of 49 nt and 34 nt respectively were designed. Both of them persists the key stem-loop motif including nucleotides 14-18 and 26-29 and some adjacent sequence (Fig. 4A). Ap 32-1 mainly deleted the nucleotides from 5'-terminal and 3'-terminal of Ap 32,

whereas kept two stem-loop motifs. Ap 32-2 further removed a stem-loop motif and only kept a stem-loop motif including the predicted binding sites of Ap 32. Then the dissociation constants of Ap 32-1 and Ap 32-2 were determined by using the same fluorescent assay, which is 46.77 ± 9.84 nM and 48.40 ± 6.63 nM, respectively. The non-linear regression curves of the two aptamers are shown in Fig. 4B. And the values of B_{\max} are also listed in Table S2. Both K_d values of Ap 32-1 and Ap 32-2 are similar to that of Ap 32. The results confirm the speculation that the stem-loop motif including nucleotides 14-18 and 26-29 is the key element for the binding of the aptamer to tobramycin. Thus the truncation of Ap 32 has an only negligible influence on the affinity of the aptamer. Although Ap 32-1 possesses a little higher affinity for tobramycin than Ap 32-2, the length of Ap 32-1 is apparently longer than the latter. Considering the application potential of the two aptamers, Ap 32-2 was finally chosen as the best aptamer for tobramycin.

Insert Fig. 4

Detection of tobramycin using aptamer and AuNP-based photometric assay

To verify the application potential of Ap 32-2, the widely reported AuNP-based photometric assay was carried out. ssDNA including aptamers can be adsorbed onto the surface of AuNP. Such ssDNA-coated AuNP has favorable dispersibility in a high concentration of NaCl, while bare AuNP aggregates in the same condition. Hence Ap 32-2 serves as a stabilizer of AuNP, preventing their aggregation in NaCl solution. When tobramycin exists, it binds to Ap 32-2 specifically, competitively removes the

aptamer from AuNP and subsequently triggers the aggregation of AuNP. This can be observed by bare eyes and further quantitatively determined by UV-vis spectroscopy. As shown in Fig. 5A, with the increased concentration of tobramycin, the color of AuNP in NaCl solution gradually turns from red to purple due to the aggregation of AuNP. This process was further characterized by UV-vis spectroscopy. In the absence of tobramycin, Ap 32-2 stabilized AuNP in NaCl solution exhibits a typical absorption peak at 520 nm in the UV-vis spectrum, while the absorbance at 520 nm apparently decreases with the increased concentration of tobramycin, owing to the aggregation of Ap 32-2 stripped AuNP in NaCl solution (Fig. 5B). Furthermore, the relationship between the absorbance at 520 nm in UV-vis spectra and the concentration of tobramycin was studied, and a linear relationship was found in tobramycin concentration range of 100-1400 nM (Fig. 5C). The linear regression equation is $y = -2.599e-4x + 1.02186$, $R^2 = 0.99047$, where y represents the absorbance at 520 nm, x represents the concentration of tobramycin (nM). The detection limit of 37.90 nM can be derived (S/N=3). Therefore, the screened Ap 32-2 has satisfactory performance in an AuNP-based photometric assay for tobramycin.

Insert Fig. 5

To evaluate the binding ability and application potential of Ap 32-2 in real sample detection, artificially tobramycin-contaminated honey was prepared by spiking different concentration of tobramycin into tobramycin-free honey. The honey samples were diluted ten times before detection. And then the AuNP-based photometric assay was carried out under the same condition. The recovery and relative standard

deviation (RSD) of the determinations are listed in Table 1. The results indicate that the matrix of honey samples has a very slight influence on the binding property of the aptamer and the repeatability of the detection is excellent.

Conclusion

In summary, we described an AuNP-based photometric assay for determination of tobramycin by using a newly screened and optimized ssDNA aptamer. The aptamer Ap 32-2 with the length of 34 nt was screened by using the magnetic bead-based SELEX process and truncated by rationally designed post-SELEX process. The affinity and specificity of the aptamer were characterized. Then the aptamer was used as a recognition element to detect tobramycin through AuNP-based photometric assay. The assay exhibited the visualized characteristic and the detection limit of 37.90 nM. Furthermore, the method was successfully applied to detect tobramycin in honey samples. Compared with those reported immunoassay [7], high-performance liquid chromatography [8], or capillary electrophoresis [9] based detection for tobramycin, whose linear detection range are of 0.50-8 mg.mL⁻¹, 0.93-9.34 mg.mL⁻¹, 0.3-30 µg.mL⁻¹, AuNP-based photometric assay with the help of Ap 32-2 shows a lowered detection limit for tobramycin. With excellent binding characteristics, minimized length and interferences-resistance in the detection, the screened Ap 32-2 exhibits great promise in the fields of food safety control, clinical analysis and environmental monitoring. Meanwhile, through the application of other nanomaterials with unique properties such as fluorescence or catalysis, and appropriate design of sensing

configuration, the performance of detection may be further improved.

Acknowledgements

This work was supported by the National Natural Science Foundation of China (no. 31271860) and the Fundamental Research Funds for the Central Universities (JUSRP51402A).

References

1. Bernardi PM, Barreto F, Costa TD (2017) Application of a LC–MS/MS method for evaluating lung penetration of tobramycin in rats by microdialysis. *J Pharm Biomed Anal* 134:340–345
2. Manyanga V, Elkady E, Hoogmartens J, Adams E (2013) Improved reversed phase liquid chromatographic method with pulsed electrochemical detection for tobramycin in bulk and pharmaceutical formulation. *J Pharm Anal* 3:161–167
3. Tuerk C, Gold L (1990) Systematic evolution of ligands by exponential enrichment: RNA ligands to bacteriophage T4 DNA polymerase. *Science* 249:505–510
4. González-Fernández V, de-los-Santos-álvarez N, Lobo-Castaón MJ, Miranda-Ordieres AJ, Tuón-Blanco P (2011) Impedimetric aptasensor for tobramycin detection in human serum. *Biosens Bioelectron* 26:2354–2360

5. Wu M, Kempaiah R, Huang PJ, Maheshwari V, Liu J (2011) Adsorption and desorption of DNA on graphene oxide studied by fluorescently labeled oligonucleotides. *Langmuir* 27:2731–2738
6. Shanson DC, Hinee CJ, Daniels JV (1976) Rapid microbiologic assay of tobramycin. *J Infect Dis* 134:104–109
7. Darwish IA (2003) Development of generic continuous-flow enzyme immunoassay system for analysis of aminoglycosides in serum. *J Pharm Biomed Anal* 30:1539–1548
8. Feng CH, Lin SJ, Wu HL, Chen SH (2002) Trace analysis of tobramycin in human plasma by derivatization and high-performance liquid chromatography with ultraviolet detection. *J Chromatogr B* 780:349–354
9. Fonge H, Kaale E, Govaerts C, Desmet K, Schepdael AV, Hoogmartens J (2004) Bioanalysis of tobramycin for therapeutic drug monitoring by solid-phase extraction and capillary zone electrophoresis. *J Chromatogr B* 810:313–318
10. Zheng B, Cheng S, Liu W, Michael HL, Liang HJ (2013) Small organic molecules detection based on aptamer-modified gold nanoparticles-enhanced quartz crystal microbalance with dissipation biosensor. *Anal Biochem* 438:144–149
11. Bruno JG, Richarte AM, Phillips T (2014) Preliminary Development of a DNA aptamer-magnetic bead capture electrochemical uminescence sandwich assay for brain natriuretic peptide. *Microchem J* 115:32–38

12. Strehilitz B, Nikolaus N, Stoltenburg R (2008) Protein detection with aptamer biosensors. *Sensors* 8:4296–4307
13. Hyunjun K, Shigeori T, Kyuwon K (2015) Thrombin-induced sensitivity enhancement in impedimetric detection of Hg²⁺ ion. *B Korean Chem Soc* 36:1285–1288
14. Choi J, Park SY, Hong J, Kim S, Kim YG (2016) Detection of surrogate cells presenting vaccinia virus protein by DNA aptamers. *B Korean Chem Soc* 38:123–126
15. Labib M, Zamay AS, Kolovskaya OS, Reshetneva IT, Zamay GS, Kibbee RJ, Sattar SA, Zamay TN, Berezovski MV (2012) Aptamer-based viability impedimetric sensor for bacteria. *Anal Chem* 84:8366–8369
16. Liu GQ, Yu XF, Xue F, Chen W, Ye YK, Yang XJ, Lian YQ, Yan Y, Zong K (2012) Screening and preliminary application of a DNA aptamer for rapid detection of *Salmonella* O8. *Microchim Acta* 178:237–244
17. Mann D, Reinemann C, Stoltenburg R, Strehlitz B (2005) *In vitro* selection of DNA aptamers binding ethanolamine. *Biochem Biophys Res Commun* 338:1928–1934
18. Duan Y, Gao Z, Wang L, Wang H, Zhang H, Li H (2016) Selection and identification of chloramphenicol-specific DNA aptamers by mag-SELEX. *Appl Biochem Biotechnol* 180:1644–1656
19. Darmostuk M, Rimpelova S, Gbelcova H, Ruml T (2015) Current approaches in SELEX: An update to aptamer selection technology. *Biotechnol Adv*

33:1141–1161

20. Zhou ND, Wang JY, Zhang J, Li C, Tian YP, Joseph W (2013) Selection and identification of streptomycin-specific single-stranded DNA aptamers and the application in the detection of streptomycin in honey. *Talanta* 108:109–116
21. Niazi JH, Lee SJ, Gu MK (2008) Single-stranded DNA aptamers specific for antibiotics tetracyclines. *Bioorg Med Chem* 16:7245–7253
22. Mehta J, Rouahmartin E, Van DK, Maes B, Herrebout W, Scippo ML, Dardenne F, Blust R, Robbens J (2012) Selection and characterization of PCB-binding DNA aptamers. *Anal Chem* 84:1669–1676
23. Zhang YH, You YD, Xia ZW, Han XY, Tian YP, Zhou ND (2016) Graphene oxide-based selection and identification of ofloxacin-specific single-stranded DNA aptamers. *RSC Adv* 6:540–545
24. Sun LH, Huang XC, Sun YY, Lu CH, Xu YY (2016) A label-free and signal-on electrochemical aptasensor for ultrasensitive kanamycin detection based on exonuclease recycling cleavage. *Anal. Methods* 8:726–730
25. Zheng DY, Zhu XL, Zhu XJ, Bo B, Yin YM, Li GX (2013) An electrochemical biosensor for the direct detection of oxytetracycline in mouse blood serum and urine. *Analyst* 138:1886–1990
26. Xu YY, H T, Li XQ, Sun LH, Zhang YJ, Zhang YS (2015) Colorimetric detection of kanamycin based on analyte-protected silver nanoparticles and aptamer-selective sensing mechanism. *Analytica Chimica Acta* 891:298–303
27. Ramezani M, Danesh NM, Lavaee P, Abnous K (2016) A selective and

- sensitive fluorescent aptasensor for detection of kanamycin based on catalytic recycling activity of exonuclease III and gold nanoparticles. *Sens Actuators B Chem* 222:1-7
28. Leung KH, He HZ, Chan DS, Fu WC, Leung CH, Ma CL (2013) An oligonucleotide-based switch-on luminescent probe for the detection of kanamycin in aqueous solution. *Sens Actuators B Chem* 177 :487-492
 29. Bai XJ, Hou H, Zhang BL, Tang JL (2014) Label-free detection of kanamycin using aptamer-based cantilever array sensor. *Biosens Bioelectron* 56:112-116
 30. Mao ZQ, Liu YZ, Miao P, Tang YG (2017) Adamantane derivatives functionalized gold nanoparticles for colorimetric detection of miRNA. *Part Part Syst Char* 34:1600405
 31. Jiang L, Patel DJ (1998) Solution structure of the tobramycin-RNA aptamer complex. *Nat Struct Biol* 5:769–774
 32. Song KM, Cho M, Jo H, Min K, Jeon SH, Kim T, Han MS, Ku JK, Ban C (2011) Gold nanoparticle-based colorimetric detection of kanamycin using a DNA aptamer. *Anal Biochem* 415:175–181
 33. He XQ, Guo L, He JL, Xu H, Xie JW (2017) Stepping library-based post-SELEX strategy approaching to the minimized aptamer in SPR. *Anal Chem* 89:6559–6566
 34. Hu LJ, Wang LL, Lu WW, Zhao JX, Zhang H, Chen W (2017) Selection, characterization and interaction studies of a DNA aptamer for the detection of bifidobacterium bifidum. *Int J Mol Sci* 18:883–894

35. Shangguan DH, Tang ZW, Prabodika M, Xiao ZY, Tan WH (2010) Optimization and modifications of aptamers selected from live cancer cell lines. *ChemBioChem* 8:603–606
36. Gao SH, Zheng X, Jiao BH, Wang LH (2016) Post-SELEX optimization of aptamers. *Anal Bioanal Chem* 408:4567–4573
37. Green R, Ellington AD, Szostak JW (1990) *In vitro* genetic analysis of the tetrahymena self-splicing intron. *Nature* 347:406–408
38. Wu SJ, Li Q, Duan N, Ma HL, Wang ZP (2016) DNA aptamer selection and aptamer-based fluorometric displacement assay for the hepatotoxin microcystin-RR. *Microchim Acta* 183:2555–2562
39. Müller M, Weigand JE, Weichenrieder O, Suess B (2006) Thermodynamic characterization of an engineered tetracycline-binding riboswitch. *Nucleic Acids Res* 34:2607–2617
40. Li S, Mao LY, Tian YP, Wang JY, Zhou ND (2012) Spectrophotometric detection of tyrosinase activity based on boronic acid-functionalized gold nanoparticles. *Analyst* 137:823–825

Figure Captions

Fig. 1. The recovery of tobramycin-bound ssDNA after each SELEX round.

Fig. 2. The predicted secondary structure models of tobramycin-specific aptamers (A) Ap 1; (B) Ap 11; (C) Ap 12; and (D) Ap 32 by Mfold. Green regions represent the fixed sequences and the black regions represent random sequences.

Fig. 3. The prediction of the recognition sites of Ap 32 for tobramycin by molecular docking.

Fig. 4. (A) The secondary structures of the truncated aptamers, Ap 32-1 and Ap 32-2; (B) The saturation curves of Ap 32 and the truncated Ap 32-1 and Ap 32-2.

Fig. 5. (A) Color change of AuNP in NaCl in the presence of different concentration of tobramycin; (B) UV-vis spectra of AuNP in the presence of different concentration of tobramycin; (C) The linear relationship between the absorbance of AuNP at 520 nm and the concentration of tobramycin.

Table 1. The recovery and RSD of tobramycin detection in honey samples by using AuNP-based photometric assay.

Added (nM)	Found (nM)	Recovery (%)	RSD (%)
200	196.7	98.35	3.72
400	392.4	98.10	2.18
600	586.4	97.73	3.97

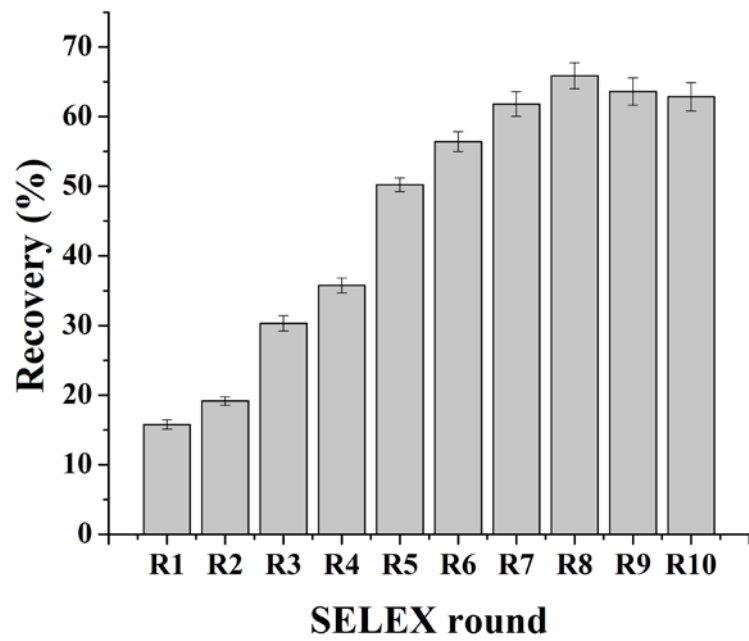


Fig. 1

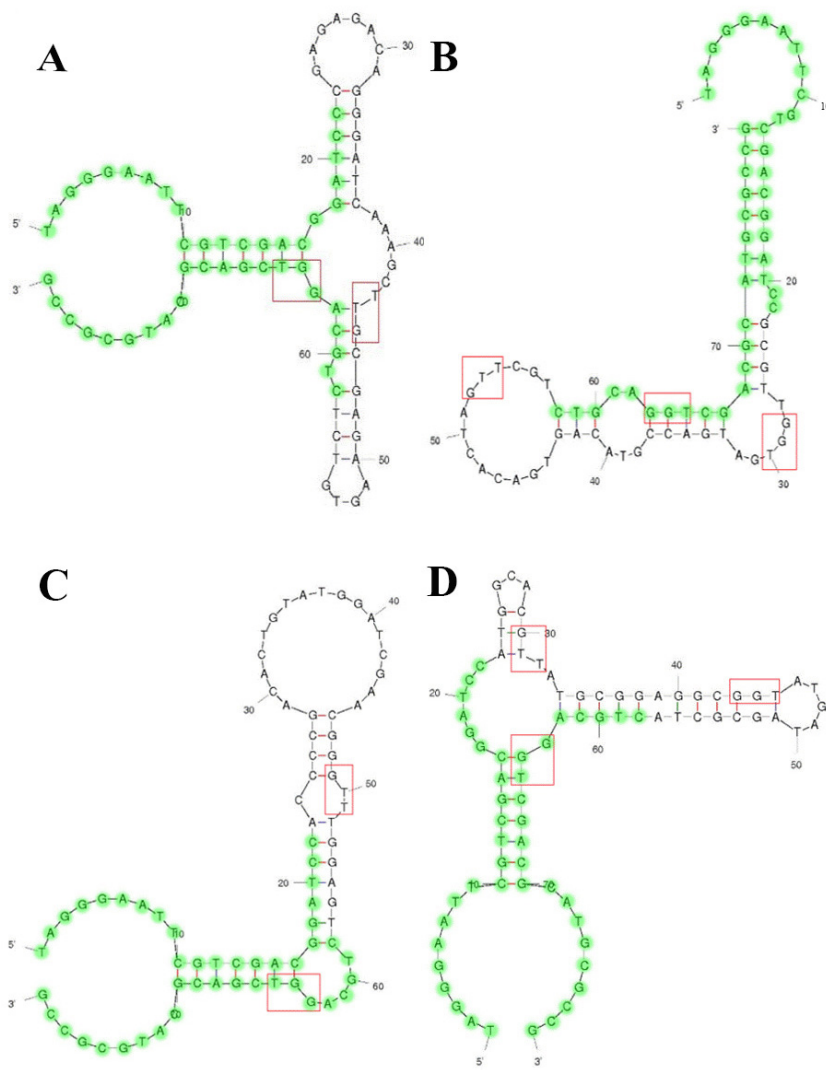


Fig. 2

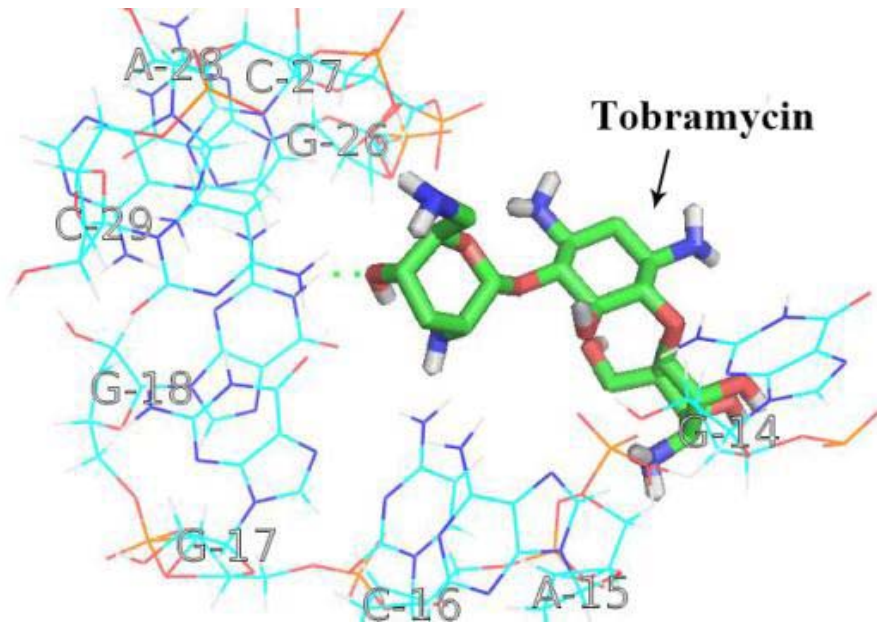


Fig. 3

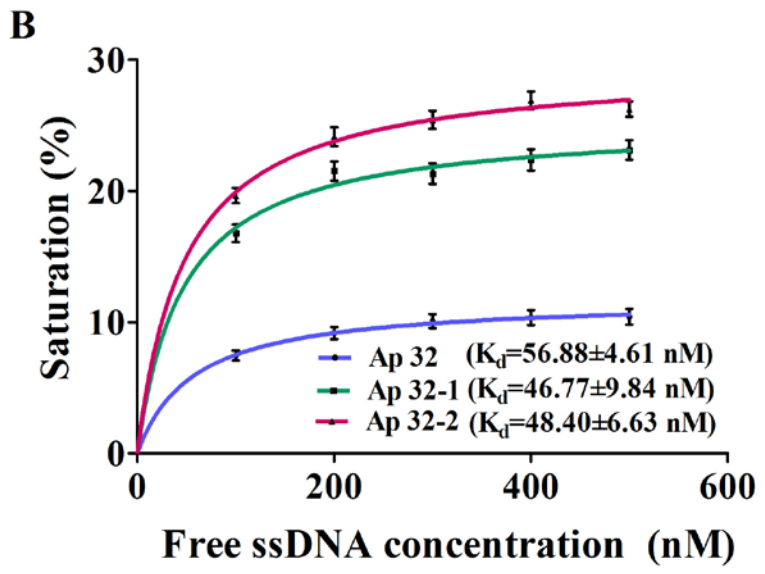
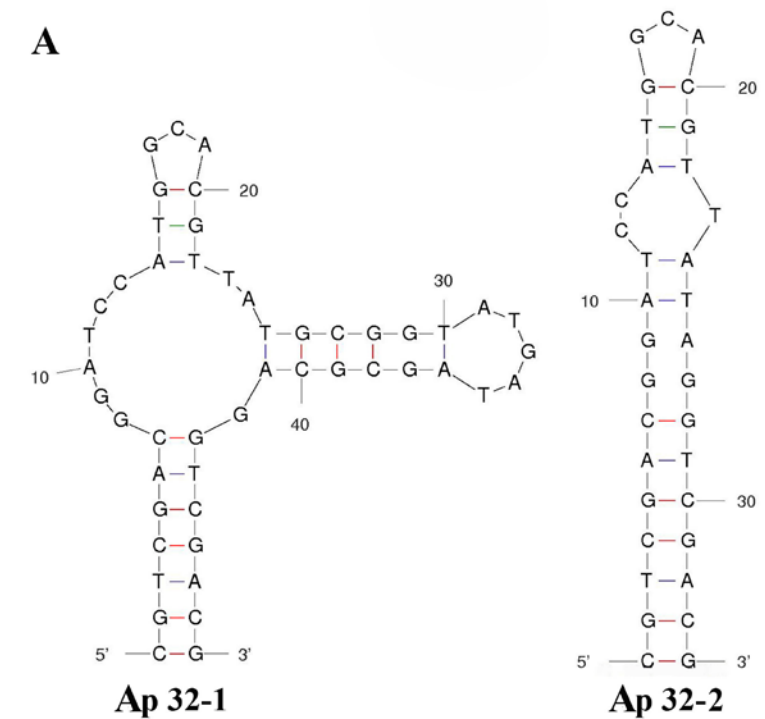


Fig. 4

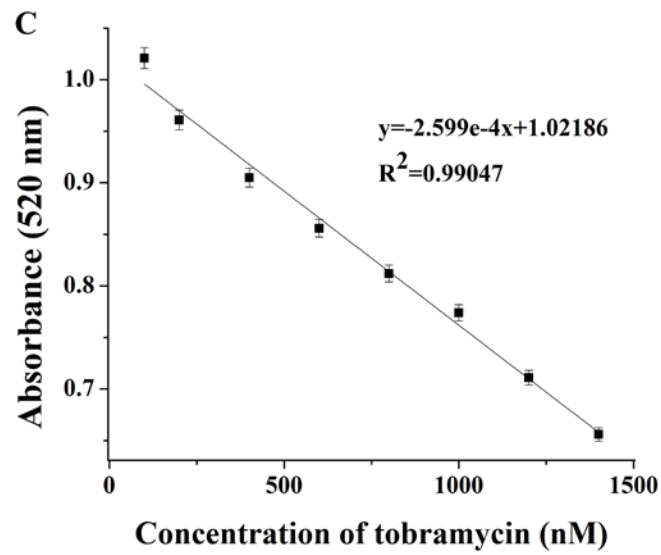
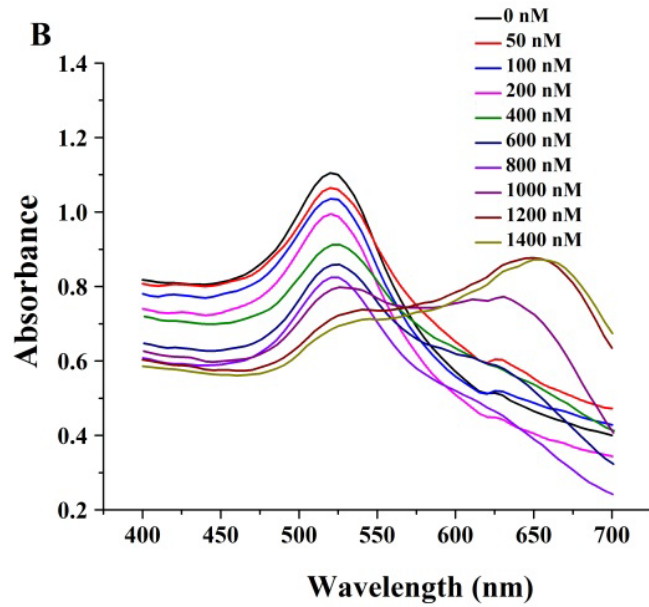


Fig . 5